Journal of Photochemistry and Photobiology A: Chemistry 219 (2011) 217–227

Contents lists available at ScienceDirect

Journal of Photochemistry and Photobiology A: Chemistry

journal homepage: www.elsevier.com/locate/jphotochem

The first comparison of photophysical and photochemical properties of non-ionic, ionic and zwitterionic gallium (III) and indium (III) phthalocyanines

Meryem Çamur[a], Vefa Ahsen[a,b], Mahmut Durmuş[a,*]

[a] *Gebze Institute of Technology, Department of Chemistry, P.O. Box 141, Gebze 41400, Kocaeli, Turkey*
[b] *Materials Institute, TUBITAK-Marmara Research Center, P.O. Box 21, Gebze 41470, Turkey*

ARTICLE INFO

Article history:
Received 26 November 2010
Received in revised form 15 February 2011
Accepted 21 February 2011
Available online 25 February 2011

Keywords:
Photodynamic therapy
Phthalocyanines
Singlet oxygen
Water soluble
Zwitterions

ABSTRACT

The spectroscopic, aggregation properties, photophysical and photochemical behaviour of 3-hydroxypyridine substituted gallium (III) and indium (III) phthalocyanine complexes and their quaternized ionic and zwitterionic derivatives are investigated and compared for the first time. The quaternized ionic and zwitterionic phthalocyanine complexes show excellent solubility in water, which makes them potential photosensitizer for use in photodynamic therapy (PDT) of cancer. Photophysical and photochemical properties of photosensitizers are very important for determination of these complexes as PDT agents. Especially, the singlet oxygen quantum yields give an indication of the efficiency of potential photosensitizers in PDT applications. The studied phthalocyanine complexes (**3**–**8**) have good singlet oxygen quantum yields. This study also presented the water soluble gallium (III) and indium (III) phthalocyanines strongly bind to blood plasma proteins such as bovine serum albumin (BSA).

1. Introduction

Photodynamic therapy (PDT) is an alternative cancer treatment which is a combination of a photosensitizing drug and light in the presence of molecular oxygen. PDT has been used to obtain a therapeutic effect, and proposed as an alternative treatment to complement conventional protocols in the management of malignant tumours and many other nononcologic diseases [1]. The use of photosensitizing agents for inactivation of several cancer cells has been widely studied [2]. An ideal photosensitizer should be chemically pure, have high efficiency of singlet oxygen generation and significant absorption at far-red and near infrared wavelengths, respectively. In addition, it should have preferential tumour localization, exhibiting good phototoxicity and low dark toxicity, and soluble in the injectable solvents such as water. The drug properties deemed favorable for PDT include synthetic purity, effectiveness at far-red and near infrared wavelengths where tissues are more transparent, and short-term photosensitization of the patient's skin [3].

The first photosensitizers are hematoporphyrin derivatives and have already been described in detail in several articles [4,5]. Second generation photosensitizers such as phthalocyanines have also been introduced for PDT in research and clinical trials [6]. To date, several phthalocyanine systems such as the silicon (IV) phthalocyanine Pc4 and a liposomal preparation of zinc (II) phthalocyanine have been in clinical trials. Photosens®, which is a mixture of sulphonated aluminium (III) phthalocyanines, is clinically used in Russia for the treatment of a range of cancers [7]. Due to their high molar absorption coefficient in the red part of the spectrum, photostability and long lifetimes of the photoexicited triplet states, phthalocyanines (Pcs) are known to be useful photosensitizers [8–10]. A decisive disadvantage of phthalocyanines is their low solubility in organic solvents or water. Altering the peripheral substitution of the macrocyclic ring is one way of tailoring the solubility properties of the Pc material. Water-soluble Pcs include sulphonates [11,12], carboxylates [13–15], phosphonates [16], and quaternized amino groups [17] on the peripheral positions. Another type of water-soluble Pcs contains hydrophilic groups as axial ligands coordinated to the central metal ion [18,19]. The methylation of the nitrogen atoms using appropriate agents (such as methylbromide, methyliodide or dimethylsulphate) is the best way for quaternization of the compounds. 1,3-Propanesultone [20] is also used for quaternization of the nitrogen atoms. This quaternization reagent bears a hidden sulphonate group that appears after the opening of the ring during the quaternization [21]. Only a few Pc molecules bearing anionic and cationic charges on the same molecule (zwitterionic) are reported [22–24]. They are generally a result of the quaternization of substituent nitrogen by 1,3-propanesultone. The advantages of Pcs bearing cationic substituents over those with neutral and anionic substituents are numerous and the cation-substituted MPcs are too noticeable to overlook [25], hence our interest in these complexes.

---

[*] Corresponding author. Tel.: +90 262 6053077; fax: +90 262 6053101.
E-mail address: durmus@gyte.edu.tr (M. Durmuş).

1010-6030/$ – see front matter © 2011 Elsevier B.V. All rights reserved.
doi:10.1016/j.jphotochem.2011.02.014

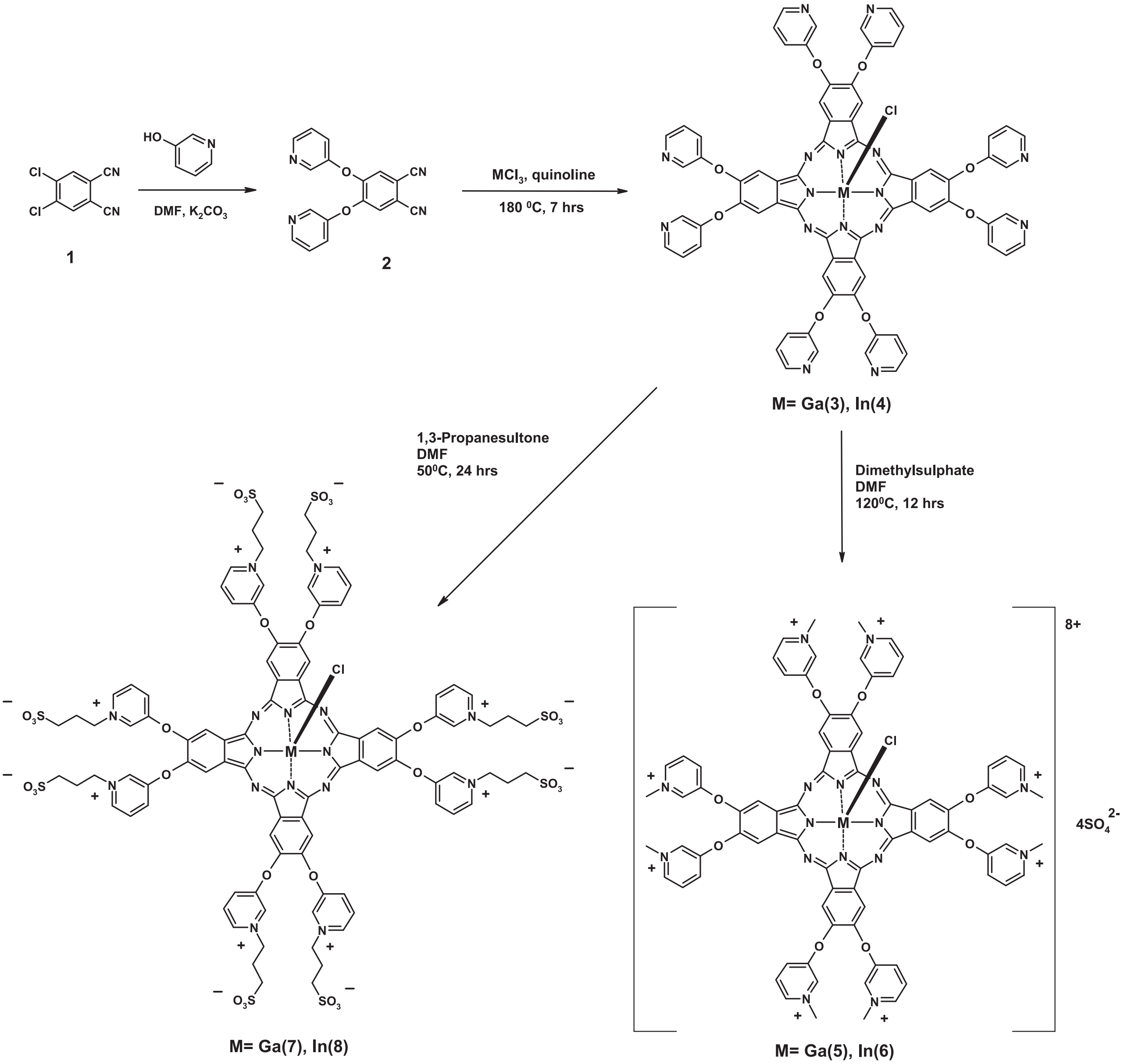

Scheme 1. Synthesis route of 3-pyridyloxy substituted gallium (III) and indium (III) Pc complexes and their quaternized ionic and zwitterionic derivatives.

The PDT properties of the Pc dyes are strongly influenced by the presence and nature of the central metal ion. Complex structure of Pc with transition metals gives short triplet lifetimes to these dyes. Closed shell and diamagnetic ions, such as Zn^{2+}, Ga^{3+} and Si^{4+}, give Pc complexes with both high triplet yields and long lifetimes [8]. Diamagnetic gallium and indium metals were selected as central metals in this study. The photophysics and photochemistry of gallium (III) and indium (III) Pc complexes are well documented [26–29].

This study is the first report on comparison of the photophysical and photochemical properties of non-ionic, quaternized ionic and zwitterionic water-soluble gallium (III) and indium (III) Pc complexes. Only a few studies on the photochemical and photophysical properties of water-soluble gallium (III) and indium (III) Pc complexes are reported [25,30,31]. The aim of our ongoing research is to synthesize water-soluble gallium (III) and indium (III) Pc complexes as potential PDT agents. In this work, the synthesis, characterization and spectroscopic behaviour as well as photophysical (fluorescence quantum yields and lifetimes) and photochemical (singlet oxygen and photodegradation quantum yields) properties of new octapyridyloxy substituted non-ionic (**3** and **4**), quaternized ionic (**5** and **6**) and zwitterionic (**7** and **8**) gallium (III) and indium (III) Pc complexes (Scheme 1) are presented. Quaternized ionic and zwitterionic compounds were shown to be excellent water soluble.

BSA and human serum albumin (HSA) are major plasma proteins, which contribute significantly to physiological functions and display effective drug delivery roles [32,33], hence the investigation of binding of drugs with albumin is of interest. A spectroscopic investigation of the binding of the water-soluble gallium (III) and indium (III) Pc complexes (**5**–**8**) to BSA is also presented in this work.

2. Experimental

2.1. Materials

Zinc (II) phthalocyanine (ZnPc) and 1,3-diphenylisobenzofuran (DPBF) were purchased from Aldrich. Anhydrous indium (III) chloride, anhydrous gallium (III) chloride, K_2CO_3, 3-hydroxypyridine, dimethylsulphate (DMS) and 9,10-antracenediyl-bis(methylene) dimalonic acid (ADMA) were purchased from Fluka. Quinoline, dimethylsulphoxide (DMSO) and dimethylformamide (DMF) were dried as described by Perrin and Armarego [34] before use. Methanol, n-hexane, chloroform ($CHCl_3$), dichloromethane (DCM), tetrahydrofuran (THF), acetone and ethanol were freshly distilled. Mixed sulphonated zinc phthalocyanine ($ZnPcS_{mix}$) [35], 4,5-dichlorophthalonitrile (**1**) [36], 4,5-bis(3-pyridyloxy)phthalonitrile (**2**) [37], 2,3-octakis-[(3-pyridyloxy)phthalocyaninato] chloroindium (III) (**4**) and its quaternized derivative (**6**) [25] were synthesized and purified according to literature procedures.

2.2. Equipment

Absorption spectra in the UV–vis region were recorded with a Shimadzu 2001 UV spectrophotometer. Fluorescence excitation and emission spectra were recorded on a Varian Eclipse spectrofluorometer using 1 cm pathlength cuvettes at room temperature. FT-IR spectra (KBr pellets) were recorded on a Bio-Rad FTS 175C FT-IR spectrometer. Positive ion and linear mode MALDI-MS of complexes were obtained in dihydroxybenzoic acid as MALDI matrix using nitrogen laser accumulating 50 laser shots using Bruker Microflex LT MALDI-TOF mass spectrometer. ^1H NMR spectra were recorded in DMSO-d_6 and D_2O solutions on a Varian 500 MHz spectrometer. Elemental analyses were obtained with a Thermo Finnigan Flash 1112 Instrument. Photo-irradiations were done using a General Electric quartz line lamp (300 W). A 600 nm glass cutoff filter (Schott) and a water filter were used to filter off ultraviolet and infrared radiations, respectively. An interference filter (Intor, 670 nm with a band width of 40 nm) was additionally placed in the light path before the sample. Light intensities were measured with a POWER MAX5100 (Molelectron Detector Incorporated) power meter.

2.3. Synthesis

2.3.1. 2,3,9,10,16,17,23,24-Octakis-[(3-pyridyloxy)phthalocyaninato]chlorogallium (III) (*3*)

A mixture of anhydrous gallium (III) chloride (0.650 g, 3.68 mmol), 4,5-bis(3-pyridyloxy)phthalonitrile (**2**) (0.500 g, 1.59 mmol) and quinoline (3 mL, doubly distilled over CaH_2) was stirred at 180 °C for 7 h under nitrogen atmosphere. After cooling, the solution was dropped in n-hexane. The green solid product was precipitated and collected by filtration and washed with n-hexane. The crude product was dissolved in DMF. After concentrating, the dark green product was precipitated with hot ethanol and washed with ethanol, acetone, $CHCl_3$, n-hexane and diethylether. Yield: 0.400 g (73%); UV/vis (DMSO): λ_{max} ($\log\varepsilon$) 365 (4.84), 619 (4.43), 684 (5.30); IR (KBr): υ_{max}/cm^{-1} 3080 (Ar–CH), 1573 (C=C), 1475, 1425, 1337, 1253, 1094 (C–O–C), 999; ^1H NMR (500 MHz, DMSO-d_6, 25 °C, TMS): δ, ppm 9.18–9.40 (8H, m, Pyridyl-H), 8.78–9.20 (8H, m, Pyridyl-H), 8.46–8.80 (8H, m, Pyridyl-H), 7.80–8.20 (8H, m, Pyridyl-H), 7.50–7.76 (8H, m, Pc-H); elemental analysis: calcd. (%) for $C_{72}H_{40}ClN_{16}O_8Ga$: C 63.48, H 2.96, N 16.45; found: C 63.22, H 2.74, N 16.49; MALDI-TOF-MS: *m*/*z*: calcd. 1361.5; found [M^+−GaCl+Na] 1279.83.

2.3.2. 2,3,9,10,16,17,23,24-Octakis-[N-methyl-(3-pyridyloxy)phthalocyaninato] chloro gallium (III) sulphate (*5*)

This complex was prepared according to the method previously reported by Smith et al. [38] Compound **3** (0.05 g, 0.037 mmol) was heated to 120 °C in freshly distilled DMF (3 mL) and excess dimethylsulphate (0.1 mL) was added dropwise. The mixture was stirred at 120 °C for 12 h. After this time, the mixture was cooled to room temperature and the product was precipitated with hot acetone and collected by filtration. The green solid product was washed successively with hot ethanol, ethyl acetate, THF, chloroform, n-hexane and diethylether. The resulting hygroscopic product was dried over phosphorous pentoxide. Yield: 0.065 g (95%); UV/vis (DMSO): λ_{max} ($\log\varepsilon$) 362 (4.80), 617 (4.45), 681 (5.34); IR (KBr): υ_{max}/cm^{-1} 3080–3052 (Ar–CH), 2960 (CH), 1586 (C=C), 1505, 1399, 1279 (S=O), 1194 (S=O), 743, 606 (S–O); ^1H NMR (500 MHz, D_2O, 25 °C, TMS): δ, ppm 9.02–9.23 (8H, m, Pyridyl-H), 8.77–9.0 (8H, m, Pyridyl-H), 8.56–8.75 (8H, m, Pyridyl-H), 8.30–8.48 (8H, m, Pyridyl-H), 7.95–8.26 (8H, m, Pc-H), 4.30 (24H, s, CH_3); elemental analysis: calcd. (%) for $C_{80}H_{72}ClN_{16}O_{28}S_4Ga$ (+$4H_2O$): C 49.55, H 3.72, N 11.56; found: C 49.41, H 3.78, N 11.68. MALDI-TOF-MS: *m*/*z*: calcd. 1865.5; found [M^+−GaCl] 1760.02.

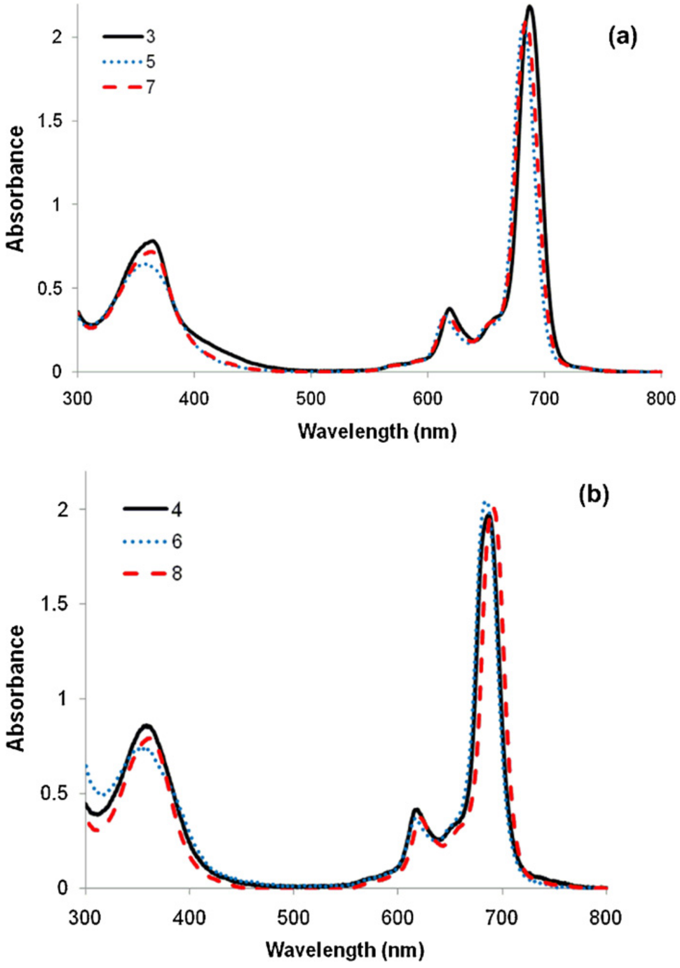

Fig. 1. Absorption spectra of (a) gallium (III) Pc complexes (**3**, **5** and **7**) and (b) indium (III) Pc complexes (**4**, **6** and **8**) in DMSO. Concentration: 1.0×10^{-5} M.

2.3.3. 2,3,9,10,16,17,23,24-Octakis-[3-(N-propanesulfonicacid)pyridyloxy] phthalocyaninato chlorogallium (III) (*7*)

Compound **3** (0.05 g, 0.037 mmol) and excess 1,3-propanesultone (0.718 g, 5.88 mmol) were dissolved in DMF (3 mL) and kept at 50 °C for 24 h under nitrogen atmosphere while stirring. The product was precipitated with CH_2Cl_2, filtered and washed with copious amounts of CH_2Cl_2 and acetone to remove excess 1,3-propanesultone. The product was dissolved in water, filtered to separate insoluble purity. Then the product was precipitated with acetone, filtered and dried over phosphorous pentoxide. Yield: 0.081 g (93%); UV/vis (DMSO): λ_{max} ($\log \varepsilon$) 367 (4.84), 620 (4.47), 682 (5.34); IR (KBr): υ_{max}/cm^{-1} 3067 (Ar–CH), 2987–2864 (CH), 1576 (C=C), 1508, 1338, 1155 (S=O, ν_{as}), 1098 (S=O, ν_{sym}), 1045, 964, 895; ^{1}H NMR (500 MHz, D_2O, 25 °C, TMS): δ, ppm 8.91–9.23 (16H, m, Pyridyl-H), 8.62–8.84 (8H, m, Pyridyl-H), 8.32–8.55 (8H, m, Pyridyl-H), 8.02–8.20 (8H, m, Pc-H), 3.62 (16H, t, –N–CH_2–), 3.42 (16H, t, –CH_2–SO_3), 2.70–3.05 (16H, m, –CH_2–); elemental analysis: calcd. (%) for $C_{96}H_{88}ClN_{16}O_{32}S_8Ga$: C 49.29, H 3.79, N 9.58; found: C 49.36, H 3.71, N 9.49; MALDI-TOF-MS: *m*/*z*: calcd. 2337.5; found [M$^+$−4(H_2SO_3)−2($C_3H_6SO_3$)] 1765.02, [M$^+$−4(H_2SO_3)−3($C_3H_6SO_3$)+Na] 1667.10.

2.3.4. 2,3,9,10,16,17,23,24-Octakis-[3-(N-propanesulfonicacid)pyridyloxy] phthalocyaninato chloroindium (III) (*8*)

Compound **4** (0.10 g, 0.07 mmol) and excess 1,3-propanesultone (1.39 g, 11.38 mmol) were dissolved in DMF (5 mL) and kept at 50 °C for 24 h under nitrogen atmosphere while stirring. The product was precipitated with CH_2Cl_2, filtered and washed with copious amounts of CH_2Cl_2 and acetone to remove excess 1,3-propanesultone. The product was dissolved in water, filtered to separate insoluble purity. Then the product was precipitated with acetone, filtered and dried over phosphorous pentoxide. Yield: 0.152 g (89%); UV/vis (DMSO): λ_{max} ($\log \varepsilon$) 366 (4.91), 626 (4.49), 689 (5.33); IR (KBr): υ_{max}/cm^{-1} 3052 (Ar–CH), 2965–2858 (CH), 1582 (C=C), 1501, 1347, 1153 (S=O, ν_{as}), 1093 (S=O, ν_{sym}), 1040, 954, 886; ^{1}H NMR (500 MHz, D_2O, 25 °C, TMS): δ, ppm 9.22–9.40 (8H, m, Pyridyl-H), 8.71–9.0 (16H, m, Pyridyl-H), 8.42–8.55 (8H, m, Pyridyl-H), 8.05–8.22 (8H, m, Pc-H), 3.71 (16H, t, –N–CH_2–), 3.51 (16H, t, –CH_2–SO_3), 2.70–3.05 (16H, m, –CH_2–); elemental analysis: calcd. (%) for $C_{96}H_{88}ClN_{16}O_{32}S_8In$: C 48.35, H 3.72, N 9.40; found: C 48.46, H 3.75, N 9.34. MALDI-TOF-MS: *m*/*z*: calcd. 2382.5; found [M$^+$−4($C_8H_{10}NSO_3$)] 1582.52.

2.4. Photophysical parameters

2.4.1. Fluorescence quantum yields and lifetimes

Fluorescence quantum yields (Φ_F) were determined by the comparative method using Eq. (1) [39]:

$$\Phi F = \Phi F(\mathrm{Std}) \frac{F \cdot A_{\mathrm{Std}} \cdot n^2}{F_{\mathrm{Std}} \cdot A \cdot n_{\mathrm{Std}}^2} \tag{1}$$

where F and F_{Std} are the areas under the fluorescence emission curves of the samples (**3**–**8**) and the standard, respectively. A and A_{Std} are the relative absorbance of the sample and standard at the excitation wavelength, respectively. n^2 and n_{Std}^2 are the refractive indices of solvents for the sample and standard, respectively. Unsubstituted ZnPc (in DMSO) ($\Phi_F = 0.20$) [40] was employed as the standard. Both the sample and standard were excited at the same wavelength. The absorbance of the solutions was ranged between 0.04 and 0.05 at the excitation wavelength.

Natural radiative lifetimes (τ_0) were determined using Photochem CAD program which uses the Strickler–Berg equation [41]. The fluorescence lifetimes (τ_F) were evaluated using Eq. (2):

$$\Phi_F = \frac{\tau_F}{\tau_0} \tag{2}$$

2.5. Photochemical parameters

2.5.1. Singlet oxygen quantum yields

Singlet oxygen quantum yields of the samples (**3**–**8**) were determined as previously explained in detail [42,43]. Typically, 2 mL portion of the samples (**3**–**8**) solutions (concentration = 1×10^{-5} M) containing the singlet oxygen quencher was irradiated in the Q band region with the photo-irradiation set-up described in Refs. [42,43]. Singlet oxygen quantum yields (Φ_Δ) were determined in air using the relative method with ZnPc (in DMSO) and $\mathrm{ZnPcS_{mix}}$ (in PBS, phosphate-buffered saline) as references; and DPBF and ADMA respectively as chemical quenchers for singlet oxygen, using Eq. (3):

$$\Phi_\Delta = \Phi_\Delta^{\mathrm{Std}} \frac{R \cdot I_{\mathrm{abs}}^{\mathrm{Std}}}{R^{\mathrm{Std}} \cdot I_{\mathrm{abs}}} \tag{3}$$

where $\Phi_\Delta^{\mathrm{Std}}$ is the singlet oxygen quantum yield for the standard {ZnPc ($\Phi_\Delta^{\mathrm{Std}} = 0.67$ in DMSO [44]) and $\mathrm{ZnPcS_{mix}}$ ($\Phi_\Delta^{\mathrm{Std}} = 0.45$ in aqueous solution [45])}; R and R^{Std} are the DPBF or ADMA photobleaching rates in the presence of the samples (**3**–**8**) and standard, respectively; I_{abs} and $I_{\mathrm{abs}}^{\mathrm{Std}}$ are the rates of light absorption by the samples (**3**–**8**) and standard, respectively. To avoid chain reactions induced by DPBF (or ADMA) in the presence of singlet oxygen [46], the concentration of quenchers (DPBF or ADMA) were lowered to ~3×10^{-5} M. Solutions of sensitizer (absorbance = 1 at the irradiation wavelength) containing quencher (DPBF or ADMA) were prepared in the dark and irradiated in the Q band region using the set-up described above. DPBF degradation at 417 nm and ADMA degradation at 380 nm were monitored. The light intensity 6.61×10^{15} photons s^{-1} cm^{-2} was used for Φ_Δ determinations.

2.5.2. Photodegradation quantum yields

Photodegradation quantum yield (Φ_d) determinations were carried out using the experimental set-up described in literature [42,43]. For determination of photodegradation quantum yields (Φ_d) Eq. (4) was employed:

$$\Phi_d = \frac{(C_0 - C_t) \cdot V \cdot N_A}{I_{\mathrm{abs}} \cdot S \cdot t} \tag{4}$$

where C_0 and C_t are the samples (**3**–**8**) concentrations before and after irradiation respectively, V, the reaction volume; S, the irradiated cell area (2.0 cm^2); t, the irradiation time; N_A, Avogadro's number and I_{abs}, the overlap integral of the radiation source intensity and the absorption of the Pc (the action spectrum) in the region of the interference filter transmittance. A light intensity of 2.20×10^{16} photons s^{-1} cm^{-2} was employed for Φ_d determinations.

2.5.3. Binding of quaternized cationic and zwitterionic gallium (III) and indium (III) Pc complexes to BSA

The binding properties of the water soluble gallium (III) and indium (III) phthalocyanine complexes (**5**–**8**) to BSA were studied by spectrofluorometry at room temperature. A PBS solution of BSA (fixed concentration) was titrated with varying concentrations of the respective phthalocyanine complex (**5**–**8**) solutions in PBS. BSA was excited at 280 nm and fluorescence recorded between 290 and 500 nm. The steady diminution in BSA fluorescence with increase in quaternized ionic or zwitterionic gallium (III) and indium (III) Pc concentrations was noted and used in the determination of the binding constants and the number of binding sites on BSA, according to Eq. (5) [47]:

$$\log \left[\frac{F_0 - F}{F - F_\infty} \right] = \log K_b + n \log[\mathrm{Pc}] \tag{5}$$

where F_0 and F are the fluorescence intensities of BSA in the absence and presence of quaternized ionic or zwitterionic Pc complexes (**5**–**8**) respectively; F_∞, the fluorescence intensity of BSA saturated with quaternized ionic or zwitterionic Pc complexes; K_b, the binding constant; n, the number of binding sites on a BSA molecule; and [Pc] the concentration of quaternized ionic or zwitterionic Pc complexes. Plots of $\log[(F_0 - F)/(F - F_\infty)]$ against log [Pc] would provide the values of n (from the slope) and K_b (from the intercept).

The changes in BSA fluorescence intensity were related to quaternized ionic or zwitterionic Pc concentrations by the Stern–Volmer relationship (Eq. (6)):

$$\frac{F_0^{\mathrm{BSA}}}{F^{\mathrm{BSA}}} = 1 + K_{\mathrm{SV}}^{\mathrm{BSA}}[\mathrm{Pc}] \tag{6}$$

and $k_{\mathrm{SV}}^{\mathrm{BSA}}$ is given by Eq. (7):

$$K_{\mathrm{SV}}^{\mathrm{BSA}} = k_{\mathrm{q}}\tau_{\mathrm{F(BSA)}} \tag{7}$$

where F_0^{BSA} and F^{BSA} are the fluorescence intensities of BSA in the absence and presence of quaternized ionic or zwitterionic Pc complexes (**5**–**8**) respectively; $K_{\mathrm{SV}}^{\mathrm{BSA}}$, the Stern–Volmer quenching constant; k_{q}, the bimolecular quenching constant; and $\tau_{\mathrm{F(BSA)}}$, the fluorescence lifetime of BSA. τ_{F}(BSA) is known to be 10 ns [48–50], thus from the values of $K_{\mathrm{SV}}^{\mathrm{BSA}}$ obtained from the plots of $F_0^{\mathrm{BSA}}/F^{\mathrm{BSA}}$ versus [Pc], the value of k_{q} may be determined using Eq. (7).

3. Results and discussion

3.1. Synthesis and characterization

The synthesis of gallium (III) Pc complex (**3**) was achieved by treatment of phthalonitrile **2** with anhydrous $\mathrm{GaCl_3}$ in freshly distilled quinoline. Treatment of the **3** with excess dimethylsulphate (DMS) as quaternization agent in DMF afforded water soluble quaternized gallium Pc complex **5** in 95% yield. The indium (III) Pc complex (**4**) and its quaternized derivative (**6**) were synthesized according to the literature [25]. Quaternization of the complexes **3** and **4** with an excess of 1,3-propanesultone led to the zwitterionic gallium (III) and indium (III) Pc complexes **7** and **8**, respectively (Scheme 1).

Generally, Pc complexes are insoluble in most organic solvents and water; however introduction of substituents on the ring increases the solubility. All studied Pc complexes **3**–**8** exhibited excellent solubility in DMF and DMSO. Quaternized and zwitterionic complexes (**5**–**8**) are soluble in water as well. The new compounds were characterized by UV/vis, IR and ^{1}H NMR spectroscopies, MALDI-TOF mass spectra and elemental analysis. The analyses are consistent with the predicted structures as shown in the experimental section. The characteristic vibrations for S–O groups at 600 $\mathrm{cm^{-1}}$ for **5** are indicative of quaternization formation. The presence of $\mathrm{SO_3}$ group gave rise to strong absorptions at 1155 $\mathrm{cm^{-1}}$ (υ_{as}, $\mathrm{SO_2}$) and 1098 $\mathrm{cm^{-1}}$ (υ_{sym}, $\mathrm{SO_2}$) for **7**; at 1153 $\mathrm{cm^{-1}}$ (υ_{as}, $\mathrm{SO_2}$) and 1093 $\mathrm{cm^{-1}}$ (υ_{sym}, $\mathrm{SO_2}$) for **8** are also indicative of formation of zwitterionic complexes.

The complexes were found to be pure by ^{1}H NMR with all the substituents and ring protons were observed in their respective regions. The Pc ring protons and pyridyl group protons were observed as unresolved multiplets between 9.40 and 7.50 ppm for complex **3** and between 9.23 and 7.95 ppm for complex **5**. The methyl protons were observed at 4.30 ppm as a singlet. The ^{1}H NMR spectrum of **7** and **8** indicated the Pc ring protons and pyridyl group protons as multiplets between 9.40 and 8.05 ppm. The aromatic protons of the complexes were shown as multiplets due to the presence of different types of aromatic protons on the molecules. In the propyl chain for **7** and **8**, $-\mathrm{N{-}CH_2}-$ protons appeared at 3.62 ppm for **7** and at 3.71 ppm for **8** as triplet, $-\mathrm{CH_2}-$ protons appeared at 2.70–3.05 ppm for both **7** and **8** as multiplets, $-\mathrm{CH_2{-}SO_3}$ protons appeared at 3.42 ppm for **7** and at 3.51 ppm for **8** as triplet. Elemental analyses results are consistent with the predicted structures. The mass spectra of **3**, **5**, **7** and **8** confirmed the proposed structures, with the molecular ion being at 1279.83 [$\mathrm{M^+{-}GaCl{+}Na}$] for **3**, 1760.02 [$\mathrm{M^+{-}GaCl}$] for **5**, 1765.02 [$\mathrm{M^+{-}4(H_2SO_3){-}2(C_3H_6SO_3)}$] for **7** and 1582.52 [$\mathrm{M^+{-}4(C_8H_{10}NSO_3)}$] for **8**.

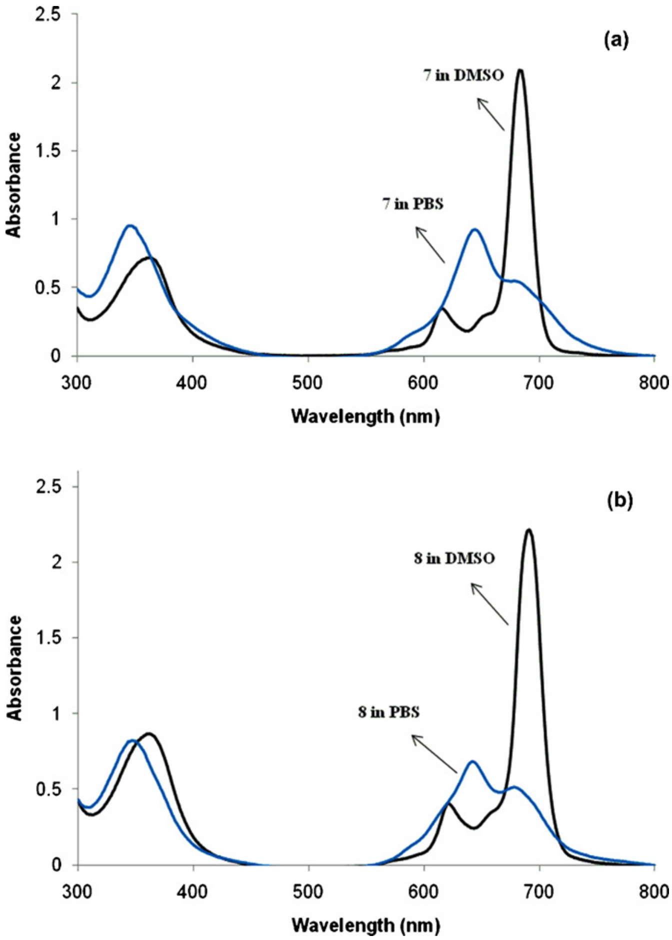

Fig. 2. Absorption spectra of (a) zwitterionic gallium (III) Pc (**7**) in DMSO and PBS, (b) zwitterionic indium (III) Pc (**8**) in DMSO and PBS. Concentration: 1.0×10^{-5} M.

3.2. UV–vis absorption and fluorescence spectra

The ground state electronic absorption spectra of gallium (**3**, **5** and **7**) and indium (**4**, **6** and **8**) Pc complexes showed monomeric behaviour evidenced by a single (narrow) Q band (at around 681–691 nm) in DMSO (Fig. 1). The B bands were observed at around 370 nm. In DMSO, the Q bands observed at 684 nm (**3**), 691 nm (**4**), 681 nm (**5**), 686 nm (**6**), 682 nm (**7**) and 689 nm (**8**), Table 1. The Q band positions of **3** and **4** in DMSO are blue-shifted by 3 or 5 nm relative to that of **5** and **6**, respectively. The lone pair electrons of the nitrogen atom of the substituent in **3** or **4** are delocalized into the ring, thereby raising the highest occupied molecular orbital (HOMO) energy, and ultimately leading to a red shifting. However, when these lone pair electrons are engaged as in quaternized complexes (**5** or **6**) and its mesomeric contribution to the ring electron density is lost. In DMSO, the zwitterionic quaternization also caused 2 or 3 nm blue-shifts for **7** and **8**, respectively. In PBS, the absorption spectra of quaternized complexes (**5**–**8**) showed cofacial aggregation as evidenced by the presence of two non-vibrational peaks in the Q band region (Fig. 2, for complexes **7** and **8** as examples). The lower energy (red-shifted) bands at 685 nm for **5**, 677 nm for **6**, 685 nm for **7** and 683 nm for **8** are due to the monomeric species, while the higher energy (blue-shifted) bands at 648 nm for **5**, 643 nm for **6**, 647 nm for **7** and 645 nm for **8** is due to the aggregated species. The B bands were observed at around 350 nm in PBS.

The aggregation behaviour of the Pc complexes (**3**–**8**) was investigated at different concentrations in DMSO (Fig. 3, for complex

Table 1
Absorption, excitation and emission spectral data for nonionic, quaternized cationic and zwitterionic gallium (III) and indium (III) Pc compounds in DMSO and PBS.

Comp.	Solvent	Q band, λ_{max} (nm)	log ε	Excitation, λ_{Ex} (nm)	Emission, λ_{Em} (nm)	Stokes shift (nm)
3	DMSO	684	5.30	684	693	9
4[a]	DMSO	691	5.05	686	702	11
5	DMSO	681	5.34	678	692	11
	PBS	648, 685	4.75, 4.50	–	–	–
6	DMSO[a]	686	4.71	685	703	17
	PBS	643, 677	4.42, 4.25	–	–	–
7	DMSO	682	5.34	680	693	11
	PBS	647, 685	4.93, 4.68	–	–	–
8	DMSO	689	5.33	687	702	13
	PBS	645, 683	4.82, 4.68	–	–	–

[a] Data from Ref. [25].

7 as an example). The studied Pc complexes (**3**–**8**) did not show aggregation in DMSO. Lambert–Beer law was obeyed for all of these compounds in the concentrations ranging from 1.2×10^{-5} to 2×10^{-6} M.

Fig. 4 shows absorption, fluorescence emission and excitation spectra of Pc complexes **3**–**8** in DMSO. The quaternization of the Pc complexes caused decreasing for fluorescence emission of the studied Pc complexes. Fluorescence emission peaks were observed at 693 nm for **3**, 702 nm for 4, 692 nm for **5**, 703 nm for **6**, 693 nm for **7** and 702 nm for **8** in DMSO (Table 1). The zwitterionic indium (III) Pc complex (**8**) showed very low fluorescence in DMSO. The studied quaternized and zwitterionic Pc complexes **5**–**8** did not show fluorescence emission in PBS. The observed Stokes shifts (Table 1) were typical of MPc complexes. The excitation spectra were similar to absorption spectra and both had mirror images of the fluorescent spectra for Pc complexes (**3**–**8**) in DMSO (Fig. 4). The proximity of the wavelength of each component of the Q band absorption to the Q band maxima of the excitation spectra for Pc complexes (**3**–**8**) suggested that the nuclear configurations of the ground and excited states were similar and not affected by excitation in DMSO.

3.3. Fluorescence quantum yields and lifetimes

The fluorescence quantum yields (Φ_F) for non-ionic (**3** and **4**), quaternized ionic (**5** and **6**) and zwitterionic (**7** and **8**) Pc complexes in DMSO are given in Table 2. The Φ_F values of all studied Pc complexes **3**–**8** are typical of gallium (III) and indium (III) Pc complexes [51]. The Φ_F values of the substituted Pc complexes (**3**–**8**) are lower compared to unsubstituted gallium (III) and indium (III) Pc complexes in DMSO, which implies that the presence of the 3-pyridyloxy substituents certainly results in fluorescence quenching. The Φ_F values of complexes **3**, **5** and **7** are higher than complexes **4**, **6** and **8** because of the indium is very heavy metal, Table 2. Zwitterionic complex **7** show largest Φ_F value compared to other studied gallium (III) and indium (III) Pc complexes in DMSO.

The fluorescence lifetime (τ_F) values (Table 2) were calculated using the Strickler–Berg equation. The τ_F values of the substituted Pc complexes (**3**–**8**) are lower compared to unsubstituted gallium (III) and indium (III) Pc complexes in DMSO, suggesting more quenching by substitution. The τ_F values of complexes **3**, **5** and **7** are higher than complexes **4**, **6** and **8** because of the indium is very heavy metal, Table 2. The natural radiative lifetime (τ_0) and the rate constants for fluorescence (k_F) values of the substituted Pc complexes (**3**–**8**) in DMSO are also given in Table 2. While the τ_0 values of the studied Pc complexes (**3**–**8**) decreased, the k_F values of them increased on going from unsubstituted gallium (III) and indium (III) Pc complexes. The τ_0 values of complexes **3**, **5** and **7** are lower, but k_F values are higher than respective complexes **4**, **6** and **8** in DMSO, Table 2.

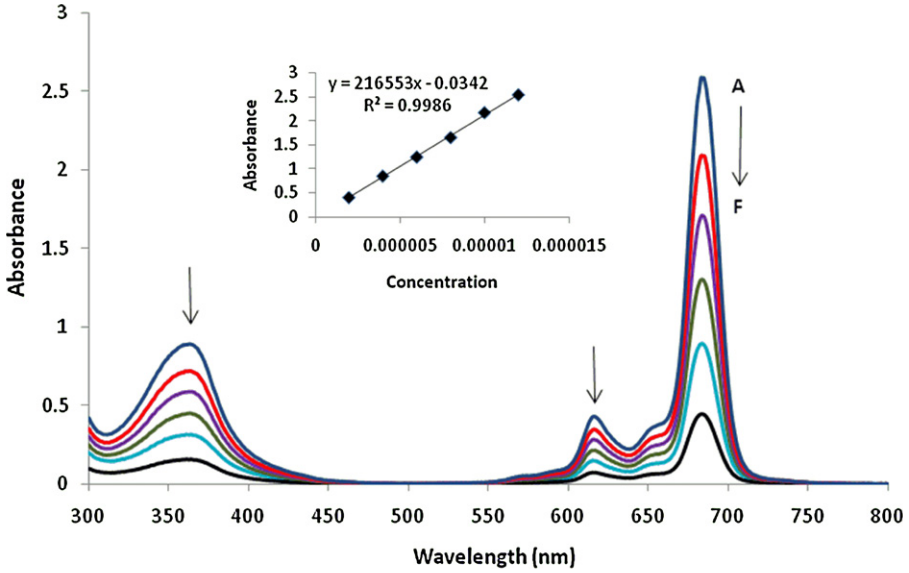

Fig. 3. Aggregation behaviour of zwitterionic gallium (III) Pc (**7**) in DMSO at different concentrations: 12×10^{-6} M (A), 10×10^{-6} M (B), 8×10^{-6} M (C), 6×10^{-6} M (D), 4×10^{-6} M (E), 2×10^{-6} M (F) (inset: plot of absorbance versus concentration).

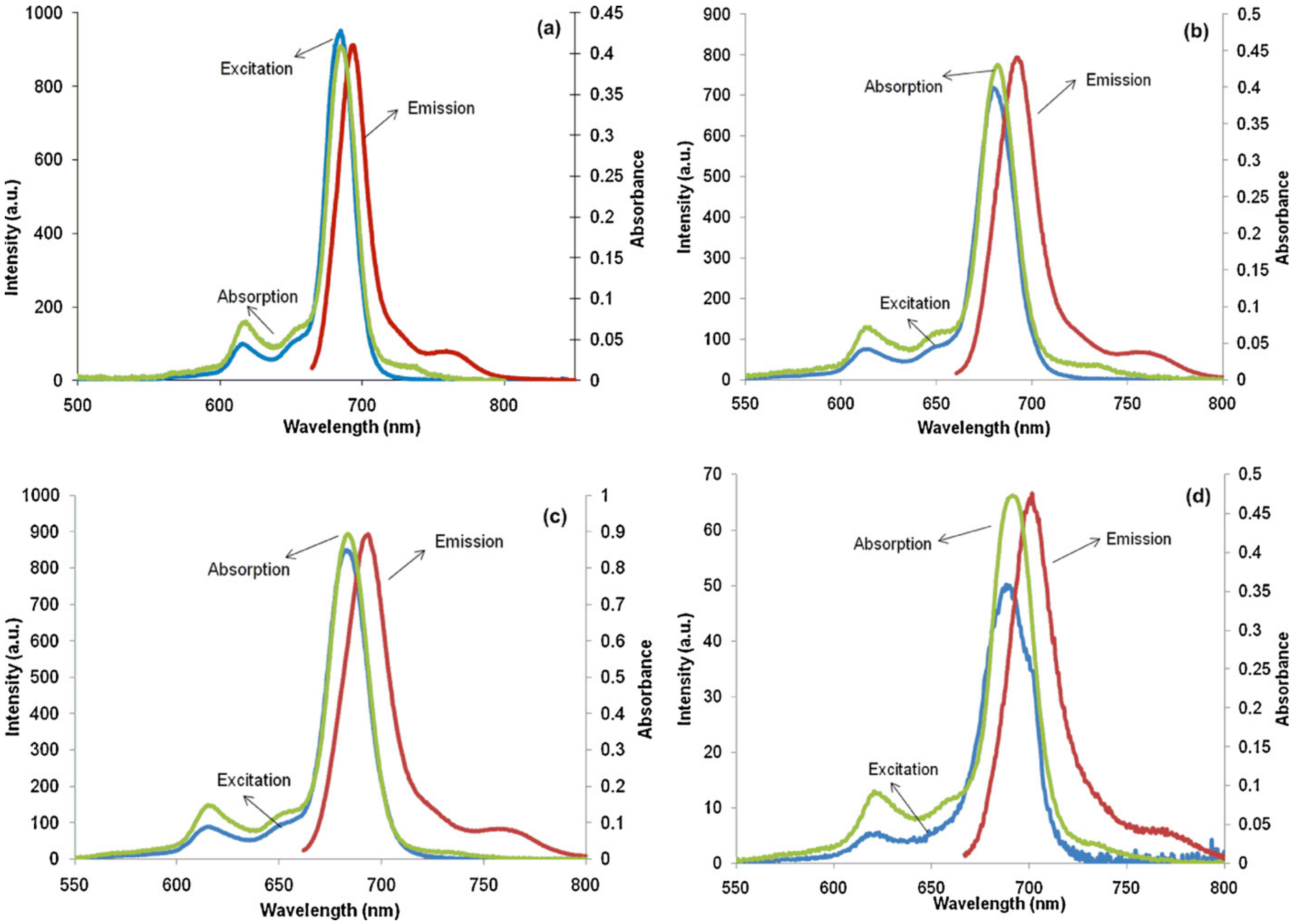

Fig. 4. Absorption, excitation and emission spectra of (a) non-ionic gallium (III) Pc (**3**) in DMSO, (b) quaternized ionic gallium (III) Pc (**5**) in DMSO, (c) zwitterionic gallium (III) Pc (**7**) in DMSO and (d) zwitterionic indium (III) Pc (**8**) in DMSO. Excitation wavelengths: 655 nm for **3**, 650 nm for **5**, 657 nm for **7** and 652 nm for **8**.

3.4. *Singlet oxygen quantum yields*

Energy transfer between the triplet state of photosensitizers and ground state molecular oxygen leads to its conversion into singlet oxygen. This transfer must be as much efficient as possible to generate large amounts of singlet oxygen. This is quantified by the singlet oxygen quantum yield (Φ_Δ), a parameter giving an indication of the potential of molecules to be used as photosensitizers in applications where singlet oxygen is required (e.g., for Type II mechanism). There is a necessity of high efficiency of transfer of energy between excited triplet state of MPc and ground state of oxygen to generate large amounts of singlet oxygen, essential for PDT. A good photosensitizer must be very efficient in generating singlet oxygen.

Table 2
Photophysical and photochemical parameters of unsubstituted, nonionic, quaternized cationic and zwitterionic gallium (III) and indium (III) Pc compounds in DMSO and PBS.

Comp.	Solvent	Φ_F	τ_F (ns)	τ_0 (ns)	k_F[a] (s^{-1}) ($\times 10^8$)	Φ_d ($\times 10^{-4}$)	Φ_Δ
3	DMSO	0.27	1.00	3.70	2.70	1.02	0.65
4[b]	DMSO	0.02	0.41	20.05	0.48	0.34	0.63
5	DMSO	0.12	0.83	6.91	1.44	2.23	0.54
	PBS	–	–	–	–	–	0.35
6	DMSO[b]	0.03	0.75	25.00	0.40	4.00	0.66
	PBS	–	–	–	–	1.84	0.15
7	DMSO	0.28	1.94	6.92	1.44	1.94	0.58
	PBS	–	–	–	–	–	0.15
8	DMSO	0.01	0.07	7.00	1.42	0.90	0.76
	PBS	–	–	–	–	0.70	0.23
GaPc[c]	DMSO	0.30	3.71	11.96	0.83	0.09	0.41
InPc[c]	DMSO	0.02	0.90	50.20	0.19	0.34	0.67

[a] k_F is the rate constant for fluorescence. Values calculated using $k_F = \Phi_F/\tau_F$.
[b] Data from Ref. [25].
[c] Data from Ref. [51].

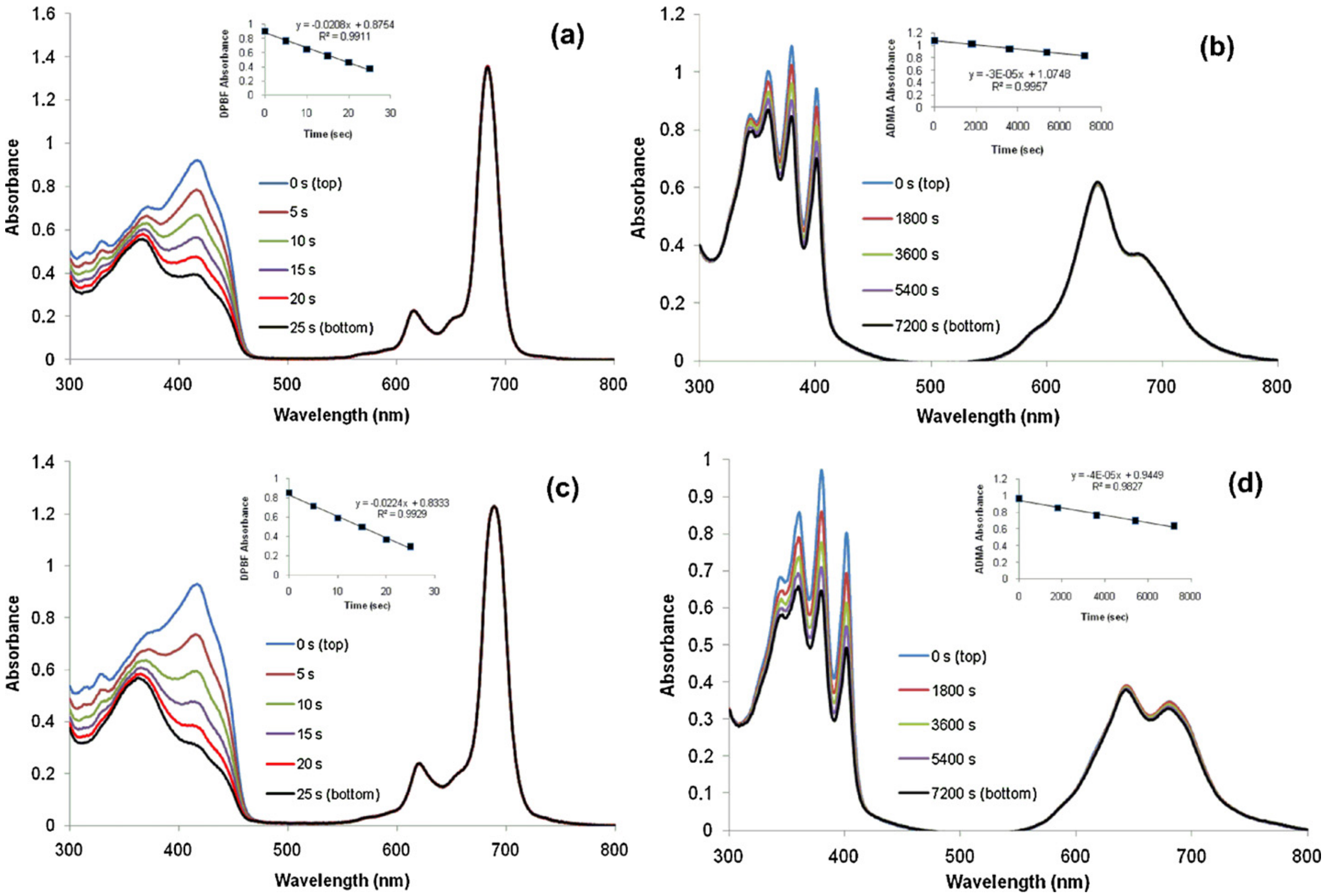

Fig. 5. A typical spectrum for the determination of singlet oxygen quantum yield of zwitterionic gallium (III) Pc (**7**) (a) in DMSO using DPBF and (b) in PBS using ADMA, zwitterionic indium (III) Pc (**8**) (c) in DMSO using DPBF and (d) in PBS using ADMA. Concentration = 1×10^{-5} M (inset: plots of DPBF or ADMA absorbance versus time).

The Φ_Δ values were determined using a chemical method (DPBF in DMSO or ADMA in PBS as singlet oxygen quenchers). The disappearance of DPBF or ADMA absorptions was monitored using UV–vis spectrophotometer (Fig. 5a using DPBF for complex **7** in DMSO, Fig. 5b using ADMA for complex **7** in PBS, Fig. 5c using DPBF for complex **8** in DMSO and Fig. 5d using ADMA for complex **8** in PBS). Many factors are responsible for the magnitude of the determined quantum yield of singlet oxygen including; triplet excited state energy, ability of substituents and solvents to quench the singlet oxygen, the triplet excited state lifetime and the efficiency of the energy transfer between the triplet excited state and the ground state of oxygen. There was no decrease in the Q band of formation of new bands during Φ_Δ determinations (Fig. 5). Table 2 shows that the values of Φ_Δ are higher for substituted complexes **3**, **5** and **7** when compared to respective unsubstituted gallium (III) Pc complex in DMSO. The values of Φ_Δ of substituted indium (III) complexes (**4** and **6**) are lower than unsubstituted indium (III) Pc complex except **8** in DMSO. Table 2 shows also that lower Φ_Δ values are observed in PBS compared to in DMSO. The low Φ_Δ in PBS (which is mainly water) compared to other solvents such as deuterated water and DMSO was explained [40] by the fact that singlet oxygen absorbs at 1270 nm, and PBS, which absorbs around this wavelength has a great effect on singlet oxygen lifetime, while DMSO which exhibits little absorption in this region has longer singlet oxygen lifetimes than PBS, resulting in large Φ_Δ values in DMSO. Low singlet oxygen values of quaternized ionic and zwitterionic gallium (III) and indium (III) Pc complexes (**5**–**8**) in PBS could also be due to aggregation. While the quaternized ionic and zwitterionic complexes **5** and **7** showed lower Φ_Δ values when compared to corresponding non-ionic complex (**3**), the quaternized and zwitterionic indium (III) Pc complexes (**6** and **8**) showed higher Φ_Δ values than non-ionic indium Pc complex (**4**) in DMSO. The Φ_Δ values of indium (III) Pc complex (in both of DMSO and PBS) are higher than gallium (III) Pc complexes because of heavy metal effect of the large indium metal.

3.5. Photodegradation studies

Degradation of the molecules under irradiation can be used to study their stability and this is especially important for those molecules intended for use in photocatalysis. The collapse of the absorption spectra without any distortion of the shape confirms clean photodegradation not associated with phototransformation into different forms of MPc absorbing in the visible region.

Fig. 6 (for complexes **5** and **8** as examples) shows changes in spectra following photodegradation. The spectral changes involved a decrease in the Q band and an increase in the absorption near 590 nm, suggesting that this band is due to reduction products of the complexes (Fig. 6a). These spectral changes were only observed in DMSO for all studied complexes (Fig. 6a as an example for complex **5** in DMSO). The first ring reduction in MPc complexes is characterized by a decrease in the Q band and the formation of weak bands between 500 and 600 nm [52]. During photodegradation, the gallium (III) and indium (III) Pc complexes were partly transformed to an anion (Pc^{3-}) species in DMSO. This type of transformation has been observed before during the photodegradation of gallium (III)

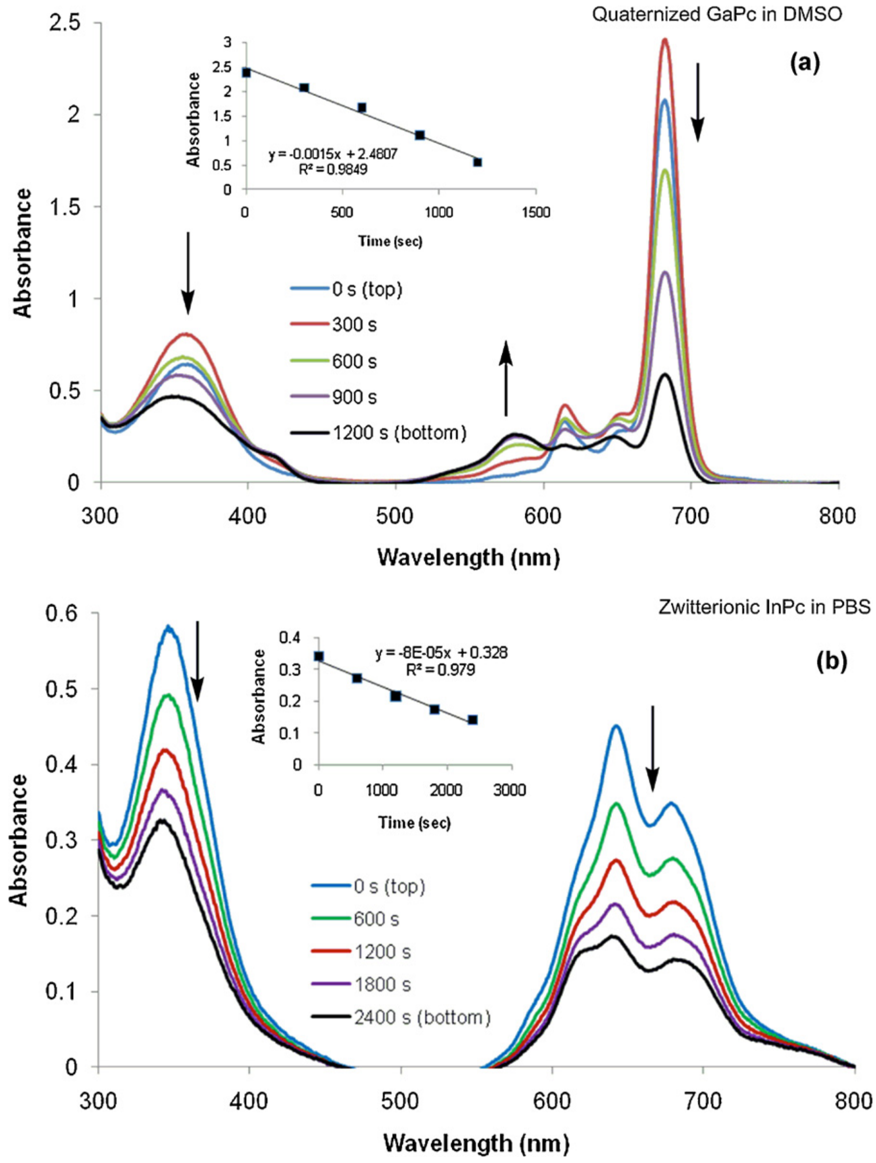

Fig. 6. The photodegradation of (a) quaternized ionic gallium (III) Pc (**5**) in DMSO and (b) zwitterionic indium (III) Pc (**8**) in PBS (inset: plot of Q band absorbance versus time).

and indium (III) Pc complexes [53]. The ionic and zwitterionic complexes **6** and **8** showed degradation without phototransformation (Fig. 6b, for complex **8** as an example) in PBS. Surprisingly, the quaternized cationic and zwitterionic complexes **5** and **7** did not show degradation in studied circumstances in PBS.

All the studied Pc complexes showed about the same stability with Φ_d of the order of 10^{-4}. The Φ_d values, found in this study for substituted gallium (III) and indium (III) Pc complexes, are higher than unsubstituted gallium (III) and indium (III) Pc complexes in DMSO. The Φ_d values are similar gallium (III) and indium (III) Pc complexes having different substituents on the Pc ring in literature [30,31,53,54]. Stable zinc Pc complexes show Φ_d values as low as 10^{-6} and for unstable molecules, values of the order of 10^{-3} have been reported [55]. It seems studied Pc complexes show also similar Φ_d values and stability with zinc Pc complexes.

3.6. Interaction of quaternized cationic and zwitterionic gallium (III) and indium (III) phthalocyanine complexes with BSA

Fig. 7 shows the fluorescence emission spectra of BSA in the presence of different concentrations of zwitterionic complex **7** in

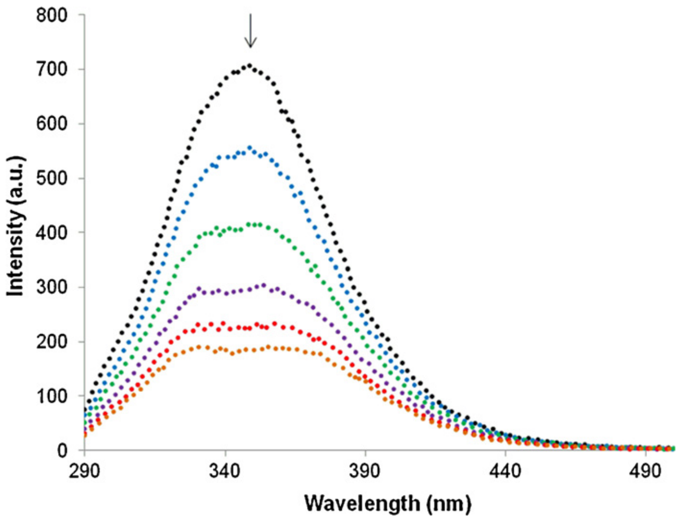

Fig. 7. Fluorescence emission spectral changes of BSA on addition of varying concentrations of zwitterionic gallium (III) Pc (**7**) in PBS. [BSA] = 3.00×10^{-5} M [7] varies from 0 to 8.30×10^{-6} M. Excitation wavelength = 280 nm.

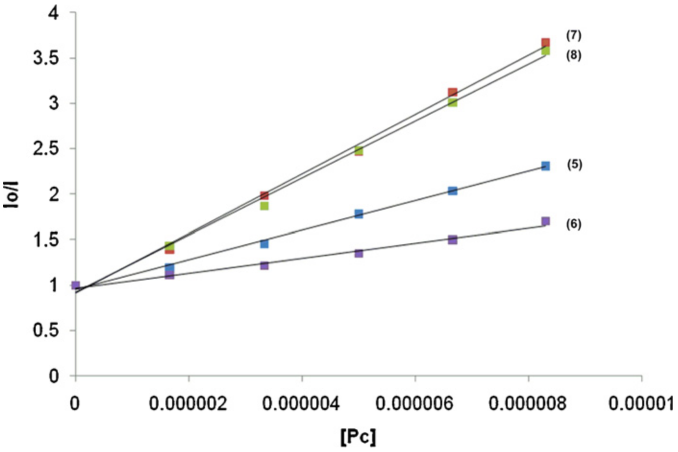

Fig. 8. Stern–Volmer plots of water soluble gallium (III) (**5** and **7**) and indium (III) Pc complexes (**6** and **8**) quenching of BSA in PBS. [BSA] = 3.00 × 10^{-5} M, [Pc] varies from 0 to 8.30 × 10^{-6} M.

Table 3
Binding and fluorescence quenching data for interaction of BSA with quaternized cationic and zwitterionic gallium (III) and indium (III) Pc compounds in PBS.

Comp.	Solvent	$K_{SV}^{BSA}/10^5$ (M^{-1})	$k_q/10^{13}$ ($M^{-1}\,s^{-1}$)	$K_b/10^{-6}$ (M^{-1})	n
5	PBS	1.67	1.67	6.61	1.22
6	PBS	0.83	0.83	12.02	1.11
7	PBS	3.44	3.44	3.80	1.28
8	PBS	3.48	3.48	4.37	1.27

PBS as an example. The BSA fluorescence at 348 nm is mainly attributable to tryptophan residues in the macromolecule. BSA and the respective quaternized ionic Pc complexes exhibit reciprocated fluorescence quenching on one another; hence it was possible to determine Stern–Volmer quenching constants (K_{SV}). The slope of the plots shown at Fig. 8 gave K_{SV} values and listed in Table 3, suggest that BSA fluorescence quenching is more effective for zwitterionic Pc complexes (**7** and **8**) than quaternized ionic Pc complexes (**5** and **6**) in PBS. Using the approximate fluorescence lifetime of BSA (10 ns) [48–50], the bimolecular quenching constant (k_q) was determined using Eq. (7). These values are of the order of 10^{13} $M^{-1}\,s^{-1}$, which exceed the proposed value of 10^{10} $M^{-1}\,s^{-1}$ for diffusion-controlled (dynamic) quenching (according to the Einstein–Smoluchowski approximation) at room temperature [56]. This also, is an indication that the mechanism of BSA quenching by quaternized or zwitterionic Pc complexes (**5**–**8**) is not diffusion-controlled (i.e., not dynamic quenching, but static quenching). The k_q values are higher for zwitterionic Pc complexes (**7** and **8**) than quaternized ionic Pc complexes (**5** and **6**) in PBS. The binding constants (K_b) and number of binding sites (n) on BSA were obtained using Eq. (5) and the results are shown in Table 3. The slope of the plots shown at Fig. 9 gave n values and the intercepts of these plots gave K_b values. The values of K_b and n are typical of MPc–BSA interactions in aqueous solutions [57]. The higher K_b value for quaternized ionic Pc complexes (**5** and **6**) implies that **5** and **6** binds more strongly to BSA than the zwitterionic Pc complexes (**7** and **8**). According to n values of near unity both gallium (III) and indium (III) Pc complexes form 1:1 adducts with BSA.

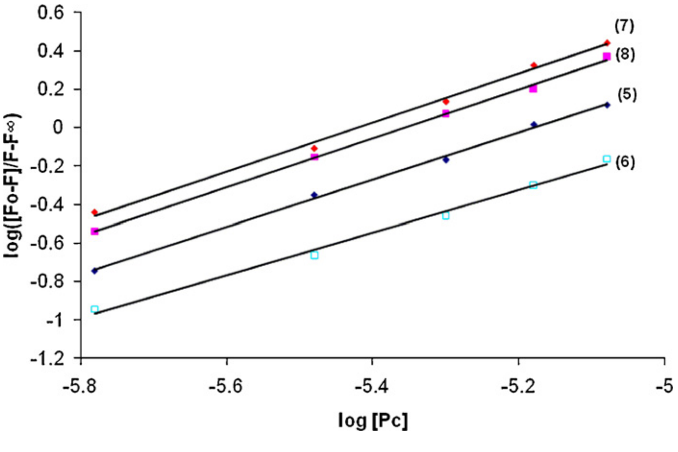

Fig. 9. Determination of Pc-BSA binding constants (K_b) and number of binding sites (n). [BSA] = 3.00 × 10^{-5} M and [Pc] varies from 0 to 8.30 × 10^{-6} M.

4. Conclusion

This work described the synthesis, spectral, photophysical and photochemical properties of new octa-pyridyloxy substituted non-ionic, quaternized ionic and zwitterionic gallium (III) and indium (III) Pc complexes. The photophysical and photochemical properties of the zwitterionic phthalocyanine complexes were reported and these properties are compared with respective non-ionic and quaternized ionic derivatives at the first time. It was shown that ionization imparted water solubility and enhanced the photophysical and photochemical value of the quaternized ionic or zwitterionic Pc complexes. Solvent effect (DMSO or PBS) on the photophysical and photochemical properties of the quaternized ionic and zwitterionic complexes was determined. The non-ionic, quaternized ionic and zwitterionic gallium (III) and indium (III) Pc complexes were found to be monomeric in DMSO. The ionic and zwitterionic complexes showed aggregation in PBS. All studied gallium (III) Pc complexes (**3**, **5** and **7**) showed similar fluorescence behaviour with MPcs. The low fluorescence emission of the indium (III) Pc complexes could be due to the larger indium metal being more displaced from the core of the Pc ring and Φ_F values of the indium (III) Pc complexes are also very low due to this effect. The substituted complexes (**3**–**8**) have good singlet oxygen quantum yields (Φ_Δ), especially complex **8** result in the highest value in DMSO. The value of Φ_Δ ranged from 0.54 to 0.76 in DMSO and from 0.15 to 0.35 in PBS gives an indication of the potential of these complexes as photosensitizers for PDT of cancer. Although, the photophysical and photochemical properties relevant for photosensitization gave more attractive values in DMSO, the values as observed in PBS could prove sufficiently high in view of potential for PDT applications. This study reveals that the water-soluble derivatives bind strongly to serum albumin; hence they can easily be transported in the blood. After injection into the blood stream, these molecules will have to encounter serum albumin, which presents a justification for their BSA binding study. This work will certainly enrich the hitherto scanty literature on the potentials of water soluble ionic and zwitterionic phthalocyanines as photosensitizers in PDT.

Acknowledgement

This study was supported by Gebze Institute of Technology (Project No. BAP-2007-A-01).

References

[1] A.C. Tedesco, J.C.G. Rotta, C.N. Lunardi, Synthesis, photophysical and photochemical aspects of phthalocyanines for photodynamic therapy, Curr. Org. Chem. 7 (2003) 187–196.
[2] J. Moan, K. Berg, Photochemotherapy of cancer: experimental research, Photochem. Photobiol. 55 (1992) 931–948.
[3] R.K. Pandey, G. Zheng, in: K. Kadish, K.M. Smith, R. Guilard (Eds.), The Porphyrin Handbook, vol. 1, Academic Press, Boston, 2003, pp. 157–230.
[4] G. Jori, Photosensitized processes in vivo: proposed phototherapeutic applications, Photochem. Photobiol. 52 (1990) 439–443.

[5] T.J. Dougherty, A brief history of clinical photodynamic therapy development at Roswell Park cancer institute, J. Clin. Laser Med. Surg. 14 (1996) 219–221.

[6] E. Ben-Hur, I. Rosenthal, Photosensitized inactivation of Chinese hamster cells by phthalocyanines, Photochem. Photobiol. 42 (1985) 129–133.

[7] C.M. Allen, W.M. Sharman, J.E. van Lier, Current status of phthalocyanines in the photodynamic therapy of cancer, J. Porphyrins Phthalocyanines 5 (2001) 161–169.

[8] H. Ali, J.E. van Lier, Metal complexes as photo- and radiosensitizers, Chem. Rev. 99 (1999) 2379–2450.

[9] D. Atilla, N. Saydan, M. Durmuş, A.G. Gürek, T. Khanc, A. Rück, H. Walt, T. Nyokong, V. Ahsen, Synthesis and photodynamic potential of tetra- and octa-triethyleneoxysulfonyl substituted zinc phthalocyanines, J. Photochem. Photobiol. A: Chem. 186 (2007) 298–307.

[10] R. Bonnett, Photosensitizers of the porphyrin and phthalocyanine series for photodynamic therapy, Chem. Soc. Rev. 24 (1995) 19–33.

[11] A. Ogunsipe, T. Nyokong, Photophysical and photochemical studies of sulphonated non-transition metal phthalocyanines in aqueous and non-aqueous media, J. Photochem. Photobiol. A: Chem. 173 (2005) 211–220.

[12] P. Kluson, M. Drobek, T. Strasak, J. Krysa, M. Karaskova, J. Rakusan, Sulphonated phthalocyanines as effective oxidation photocatalysts for visible and UV light regions, J. Mol. Catal. A: Chem. 272 (2007) 213–219.

[13] S.B. Kahl, J. Li, Synthesis and characterization of a boronated metallophthalocyanine for boron neutron capture therapy, Inorg. Chem. 35 (1996) 3878–3880.

[14] J. Chen, N. Chen, J. Huang, J. Wang, M. Huang, Derivatizable phthalocyanine with single carboxyl group: synthesis and purification, Inorg. Chem. Commun. 9 (2006) 313–315.

[15] M. Çamur, M. Bulut, Phthalocyanines prepared from 4-chloro-/4-hexylthio-5-(4-phenyloxyacetic acid)phthalonitriles and functionalization of the related phthalocyanines with hydroxymethylferrocene, J. Organomet. Chem. 695 (2010) 45–52.

[16] W.M. Sharman, S.V. Kudrevich, J.E. van Lier, Novel water-soluble phthalocyanines substituted with phosphonate moieties on the benzo rings, Tetrahedron Lett. 37 (1996) 5831–5834.

[17] M. Durmuş, V. Ahsen, Water-soluble cationic gallium(III) and indium(III) phthalocyanines for photodynamic therapy, J. Inorg. Biochem. 104 (2010) 297–309.

[18] Y.J. Zhu, J.D. Huang, X.J. Jiang, J.C. Sun, Novel silicon phthalocyanines axially modified by morpholine: synthesis, complexation with serum protein and in vitro photodynamic activity, Inorg. Chem. Commun. 9 (2006) 473–477.

[19] X.J. Jiang, J.D. Huang, Y.J. Zhu, F.X. Tang, D.K.P. Ng, J.C. Sunc, Preparation and in vitro photodynamic activities of novel axially substituted silicon (IV) phthalocyanines and their bovine serum albumin conjugates, Bioorg. Med. Chem. Lett. 16 (2006) 2450–2453.

[20] Ł. Łapok, C.G. Claessens, D. Wöhrle, T. Torres, Synthesis of water-soluble subphthalocyanines, Tetrahedron Lett. 50 (2009) 2041–2044.

[21] F. Dumoulin, M. Durmuş, V. Ahsen, T. Nyokong, Coord. Chem. Rev. 254 (2010) 2792–2847.

[22] G. Schneider, D. Wöhrle, W. Spiller, J. Stark, G. Schulz-Ekloff, Photooxidation of 2-mercaptoethanol by various water-soluble phthalocyanines in aqueous alkaline solution under irradiation with visible light, Photochem. Photobiol. 60 (1994) 333–342.

[23] M. Kaneko, H. Ueno, S. Masuda, K. Suzuki, H. Okimi, M. Hoshino, Ł. Łapok, D. Wöhrle, Quenching of singlet photoexcited state of water soluble phthalocyanines and porphyrins by viologens interacting electrostatically, J. Porphyrins Phthalocyanines 9 (2005) 667–680.

[24] Ł. Łapok, G. Schnurpfeil, R. Gerdes, S.M. Gorun, O. Suvorova, G.S. Kudryavtseva, D. Wöhrle, Synthesis of charged triazatetrabenzcorroles, phthalocyanines and tetrapyridylporphyrin, and their activities in the co-sensitized photooxidation of 2-mercaptoethanol, J. Porphyrins Phthalocyanines 3 (2009) 346–357.

[25] M. Durmuş, A. Erdoğmuş, A. Ogunsipe, T. Nyokong, The synthesis and photophysicochemical behaviour of novel water-soluble cationic indium(III) phthalocyanine, Dyes Pigments 82 (2009) 244–250.

[26] S. Wang, Q. Gan, Y. Zhang, S. Li, H. Xu, G. Yang, Optical-limiting and photophysical properties of two soluble chloroindium phthalocyanines with α- and β-alkoxyl substituents, ChemPhysChem 7 (2006) 935–941.

[27] Y. Chen, Y. Araki, D. Dini, Y. Liu, O. Ito, M. Fujitsuka, The steady-state and time-resolved photophysical properties of a dimeric indium phthalocyanine complex, Mater. Chem. Phys. 98 (2006) 212–216.

[28] Y. Chen, D. Dini, M. Hanack, M. Fujitsua, O. Ito, Excited state properties of monomeric and dimeric axially bridged indium phthalocyanines upon UV–Vis laser irradiation, Chem. Commun. (2004) 340–341.

[29] V. Chauke, M. Durmuş, T. Nyokong, Photochemistry, photophysics and nonlinear optical parameters of phenoxy and tert-butylphenoxy substituted indium(III) phthalocyanines, J. Photochem. Photobiol. A: Chem. 192 (2007) 179–187.

[30] M. Durmuş, T. Nyokong, The synthesis, fluorescence behaviour and singlet oxygen studies of new water-soluble cationic gallium(III) phthalocyanines, Inorg. Chem. Commun. 10 (2007) 332–338.

[31] M. Durmuş, T. Nyokong, Synthesis, photophysical and photochemical studies of new water-soluble indium(III) phthalocyanines, Photochem. Photobiol. Sci. 6 (2007) 659–668.

[32] D.C. Carter, J.X. Ho, Structure of serum albumin, Adv. Protein Chem. 45 (1994) 153–203.

[33] T. Peters, Serum albumin, Adv. Protein Chem. 37 (1985) 161–245.

[34] D.D. Perrin, W.L.F. Armarego, Purification of Laboratory Chemicals, second ed., Pergamon Press, Oxford, 1989.

[35] M. Ambroz, A. Beeby, M. MacRobert, M. Simpson, R. Svenson, D. Phillips, Preparative, analytical and fluorescence spectroscopic studies of sulphonated aluminium phthalocyanine photosensitizers, J. Photochem Photobiol. B: Biol. 9 (1991) 87–95.

[36] D. Wöhrle, M. Eskes, K. Shigehara, A. Yamada, A simple synthesis of 4,5-disubstituted 1,2-dicyanobenzenes and 2,3,9,10,16,17,23,24-octasubstituted phthalocyanines, Synthesis (1993) 194–196.

[37] H. Li, T.J. Jensen, F.R. Fronczek, M.G.H. Vicente, Syntheses and properties of a series of cationic water-soluble phthalocyanines, J. Med. Chem. 51 (2008) 502–511.

[38] T.D. Smith, J. Livorness, H. Taylor, J.R. Pilbrow, G.R. Sinclair, Physico-chemical study of copper(II) and cobalt(II) chelates of tetra-2,3-pyridinoporphyrazine, J. Chem. Soc. Dalton Trans. (1983) 1391–1400.

[39] D. Maree, T. Nyokong, K. Suhling, D. Phillips, Effects of axial ligands on the photophysical properties of silicon octaphenoxyphthalocyanine, J. Porphyrins Phthalocyanines 6 (2002) 373–376.

[40] A. Ogunsipe, J.-Y. Chen, T. Nyokong, Photophysical and photochemical studies of zinc(II) phthalocyanine derivatives—effects of substituents and solvents, New J. Chem. 28 (2004) 822–827.

[41] H. Du, R.A. Fuh, J. Li, A. Corkan, J.S. Lindsey, PhotochemCAD: a computer-aided design and research tool in photochemistry, Photochem. Photobiol. 68 (1998) 141–142.

[42] I. Seotsanyana-Mokhosi, N. Kuznetsova, T. Nyokong, Photochemical studies of tetra-2,3-pyridinoporphyrazines, J. Photochem. Photobiol. A: Chem. 140 (2001) 215–222.

[43] A. Ogunsipe, D. Maree, T. Nyokong, Solvent effects on the photochemical and fluorescence properties of zinc phthalocyanine derivatives, J. Mol. Struct. 650 (2003) 131–140.

[44] N. Kuznetsova, N. Gretsova, E. Kalmkova, E. Makarova, S. Dashkevich, V. Negrimovskii, O. Kaliya, E. Luk'yanets, Relationship between the photochemical properties and structure of pophyrins and related compounds, Russ. J. Gen. Chem. 70 (2000) 133–140.

[45] F. Wilkinson, W.P. Helman, A.B. Ross, Quantum yields for the photosensitized formation of the lowest electronically excited singlet state of molecular oxygen in solution, J. Phys. Chem. Ref. Data 22 (1993) 113–262.

[46] W. Splliler, H. Kliesch, W. Wöhrle, S. Hackbarth, B. Röder, G. Schnurpfeil, Singlet oxygen quantum yields of different photosensitizers in polar solvents and micellar solutions, J. Porphyrins Phthalocyanines 2 (1998) 145–158.

[47] D.M. Chipman, V. Grisaro, N. Shanon, The binding of oligosaccharides containing *N*-acetylglucosamine and *N*-acetylmuramic acid to lysozyme: the specificity of binding subsites, J. Biol. Chem. 242 (1967) 4388–4394.

[48] C.Q. Jiang, M.X. Gao, J.X. He, Study of the interaction between terazosin and serum album synchronous fluorescence determination of terazosin, Anal. Chim. Acta 452 (2002) 185–189.

[49] M. Gou, J.W. Zou, P.G. Yi, Z.C. Shang, G.X. Hu, Q.S. Yu, Binding interaction of gatifloxacin with bovine serum albumin, Anal. Sci. 20 (2004) 465–470.

[50] Z. Bıyıklıoğlu, M. Durmuş, H. Kantekin, Synthesis, photophysical and photochemical properties of quinoline substituted zinc (II) phthalocyanines and their quaternized derivatives, J. Photochem. Photobiol. A: Chem. 211 (2010) 32–41.

[51] H. Yanık, D. Aydın, M. Durmuş, V. Ahsen, Peripheral and non-peripheral tetrasubstituted aluminium, gallium and indium phthalocyanines: synthesis, photophysics and photochemistry, J. Photochem. Photobiol. A: Chem. 206 (2009) 18–26.

[52] M.J. Stillman, in: C.C. Leznoff, A.B.P. Lever (Eds.), Phthalocyanines: Properties and Applications, vol. 3, VCH Publishers, New York, 1994 (Chapter 5).

[53] M. Durmuş, T. Nyokong, Synthesis, photophysical and photochemical properties of aryloxy tetra-substituted gallium and indium phthalocyanine derivatives, Tetrahedron 63 (2007) 1385–1394.

[54] A Ogunsipe, M. Durmuş, T. Nyokong, Photophysical, photochemical and bovine serum albumin binding studies on water-soluble gallium(III) phthalocyanine derivatives, J. Porphyrins Phthalocyanines 11 (2007) 635–644.

[55] T. Nyokong, Effects of substituents on the photochemical and photophysical properties of main group metal phthalocyanines, Coord. Chem. Rev. 251 (2007) 1707–1722.

[56] S.L. Murov, I. Carmichael, G.L. Hug, Handbook of Photochemistry, Marcel Dekker Inc, New York, 1993.

[57] S.M.T. Nunes, F.S. Sguilla, A.C. Tedesco, Photophysical studies of zinc phthalocyanine and chloroaluminum phthalocyanine incorporated into liposomes in the presence of additives, Braz. J. Med. Biol. Res. 37 (2004) 273–284.